Studying Brain Morphometry using Conformal Equivalence Class

Yalin Wang
Dept of Neurology/Math
UCLA
ylwang@math.ucla.edu

Wei Dai
Dept of Math
Zhejiang Univ
dw0426@zju.edu.cn

Yi-Yu Chou
Dept of Neurology
UCLA
yiyu.chou@loni.ucla.edu

Xianfeng Gu
Dept of Comp Sci
Stony Brook Univ
gu@cs.sunysb.edu

Tony F. Chan
Dept of Math
UCLA
chan@math.ucla.edu

Arthur W. Toga
Dept of Neurology
UCLA
toga@loni.ucla.edu

Paul M. Thompson
Dept of Neurology
UCLA
thompson@loni.ucla.edu

Abstract

Two surfaces are conformally equivalent if there exists a bijective angle-preserving map between them. The Teichmüller space for surfaces with the same topology is a finite-dimensional manifold, where each point represents a conformal equivalence class, and the conformal map is homotopic to the identity map. In this paper, we propose a novel method to apply conformal equivalence based shape index to study brain morphometry. The shape index is defined based on Teichmüller space coordinates. It is intrinsic, and invariant under conformal transformations, rigid motions and scaling. It is also simple to compute; no registration of surfaces is needed. Using the Yamabe flow method, we can conformally map a genus-zero open boundary surface to the Poincaré disk. The shape indices that we compute are the lengths of a special set of geodesics under hyperbolic metric. By computing and studying this shape index and its statistical behavior, we can analyze differences in anatomical morphometry due to disease or development. Study on twin lateral ventricular surface data shows it may help detect generic influence on lateral ventricular shapes. In leave-one-out validation tests, we achieved 100% accurate classification (versus only 68% accuracy for volume measures) in distinguishing 11 *HIV/AIDS individuals from* 8 *healthy control subjects, based on Teichmüller coordinates for lateral ventricular surfaces extracted from their 3D MRI scans.Our conformal invariants, the Teichmüller coordinates, successfully classified all lateral ventricular surfaces, showing their promise for analyzing anatomical surface morphometry.*

1. Introduction

3D Surface shape analysis is a key research topic in face recognition [12], anatomical modeling, statistical comparisons of anatomy and medical image registration. In research studies that analyze brain morphometry, many shape analysis methods have been proposed, such as spherical harmonic analysis (SPHARM) [4], medial representations (M-reps) [14], and minimum description length approaches [5], etc.; these methods may be applied to analyze shape changes or abnormalities in subcortical brain structures. Even so, a stable method to compute transformation-invariant shape descriptors would be highly advantageous in this research field. Here we propose a novel and intrinsic method to compute a Teichmüller space coordinate (shape indices) and we apply it to study brain morphometry in Alzheimers disease (AD), Williams syndrome (WS) and HIV/AIDS. Our Teichmüller space coordinates are based on the surface conformal structure and can be accurately computed using the Yamabe flow method.

According to Klein's Erlangen program, different geometries study the invariants under different transformation groups. Conformal geometry corresponds to the angle-preserving transformations. If there exists a conformal map between two surfaces, they are conformally equivalent. All surfaces can be classified by the conformal equivalence relation. For surfaces with the same topology, the Teichmüller space is a natural finite-dimensional manifold, where each point represents a conformal equivalence class and the distance between two shapes can be accurately measured. A shape index can be defined based on Teichmüller space coordinates. This shape index is intrinsic, and invariant under conformal transformations, rigid motions and scaling. It is simple to compute; no surface registration is needed. It is very general; it can handle all arbitrary topology surfaces

with negative Euler numbers. By computing and studying Teichmüller space coordinates and their statistical behavior, we can provide a promising approach to describe local changes or abnormalities in anatomical morphometry due to disease or development.

In this work, we propose to study the Teichmüller space coordinate based shape index with genus-zero surfaces with three boundaries. With the discrete version of the surface Ricci flow method (also called the discrete Yamabe flow), we conformally projected the surfaces to the hyperbolic plane and isometrically embedded them in the Poincaré disk. The proposed Teichmüller space coordinates are the lengths of a special set of geodesics under this special hyperbolic metric. For applications in brain morphometry research, we first converted a closed 3D surface model of the cerebral cortex into a multiple-boundary surface by cutting it along selected anatomical landmark curves. Secondly, we conformally parameterized each cortical surface using the Yamabe flow method. Next, we computed the Teichmüller space coordinates - the lengths of three boundaries (geodesics) on the hyperbolic space - as a 3×1 feature vector. This measure is invariant in the hyperbolic plane under conformal transformations of the original surface, and is the same for surfaces that differ at most by a rigid motion.

We tested our algorithm on cortical and lateral ventricular surfaces extracted from 3D anatomical brain MRI scans. We applied our algorithm to analyze ventricular shapes in 3D volumetric MRI scans from 76 identical and 56 same-sex fraternal twins. The proposed Teichmüller space coordinate features picked up stronger generic influence than volume measures. The proposed algorithm can map the profile of differences in surface morphometry between healthy controls and subjects with HIV/AIDS. Finally, we used a nearest-neighbor classifier together with our feature vector on the lateral ventricular surface data from a group of 11 HIV/AIDS individuals and a group of 8 matched healthy control subjects. Our classifier achieved a 100% accuracy rate and outperformed a nearest neighbor classifier based on total brain volume, which achieved an overall 68.42% accuracy rate on the same dataset.

Our major contributions in this work include: a way to compute a new conformal equivalence based shape index, the Teichmüller space coordinate, on the Poincaré disk in the parameter domain of a surface. Our proposed singularity-free Yamabe flow method preserves this invariant very well, so our method offers a stable way to calculate it in 2D parametric coordinates. To the best of our knowledge, it is the first work to apply the Teichmüller space coordinate to brain morphometry research. We treated the Teichmüller space coordinates as a random vector; by calculating the Mahalanobis distance from any vector to individual members of two groups of subjects, our method achieved a 100% accuracy rate in classifying the lateral ventricular surfaces of HIV/AIDS individuals versus matched healthy control subjects. Our work may inspire more researchers to adopt conformal invariant based shape analysis in their own research.

1.1. Related Work

In the computational analysis of brain anatomy, volumetric measures of structures identified on 3D MRI have been used to study group differences in brain structure and also to predict diagnosis [1]. Recent work has also used shape-based features [13], analyzing surface changes using pointwise displacements of surface meshes, local deformation tensors, or surface expansion factors, such as the Jacobian determinant of a surface-based mapping. For closed surfaces homotopic to a sphere, spherical harmonics have commonly been used for shape analysis, as have their generalizations, e.g., eigenfunctions of the Laplace-Beltrami operator in a system of spherical coordinates. These shape indices are also rotation invariant, i.e., their values do not depend on the orientation of the surface in space. Shape analysis based on spherical harmonic basis functions (SPHARM) is usually conducted in three steps, based on a pre-computed spherical parameterization of the surface: (1) estimating SH coefficients for the x, y and z-components with a least-squares procedure, (2) normalizing the orientation of the first-order ellipsoid, and (3) reconstructing the surface at regularly spaced points on the sphere [16]. Chung et al. [4] proposed a weighted spherical harmonic representation. For a specific choice of weights, the weighted SPHARM is shown to be the least squares approximation to the solution of an anisotropic heat diffusion on the unit sphere. Davies et al. studied anatomical shape abnormalities in schizophrenia, using the minimal distance length approach to statistically align hippocampal parameterizations [5]. For classification, Linear Discriminant Analysis (LDA) or principal geodesic analysis can be used to find the best discriminant vector in the feature space for distinguishing diseased subjects from controls. Gorczowski [7] presented a framework for discriminant analysis of populations of $3D$ multi-object sets. In addition to a sampled medial mesh representation, m-rep [14], they also considered pose differences as an additional statistical feature to improve the shape classification results.

With the Ricci flow method, Wang et al. [19] solved the Yamabe equation and conformally mapped the cortical surface of the brain to a Euclidean multi-hole punctured disk. Gu et al. [8] applied the surface Ricci flow method to study general 3D shape matching and registration. The hyperbolic Ricci flow has also been applied to study 3D face matching [20]. Recently, Jin et al. [11] introduced the Teichmüller shape space to index and compare general surfaces with various topologies, geometries and resolutions.

2. Theoretical Background and Definitions

This section briefly introduces the theoretic background necessary for the current work. For details, we refer readers to [10] for algebraic topology and [9] for differential geometry.

Surface Ricci curvature flow Let S be a surface embedded in $\mathbb{R}^3$. S has a Riemannian metric induced from the Euclidean metric of $\mathbb{R}^3$, denoted by $\mathbf{g}$. Suppose $u : S \to \mathbb{R}$ is a scalar function defined on S. It can be verified that $\bar{\mathbf{g}} = e^{2u}\mathbf{g}$ is also a Riemannian metric on S conformal to the original one.

The Gaussian curvatures will also be changed accordingly. The Gaussian curvature will become

$$\bar{K} = e^{-2u}(-\Delta_{\mathbf{g}} u + K),$$

where $\Delta_{\mathbf{g}}$ is the Laplacian-Beltrami operator under the original metric $\mathbf{g}$. The above equation is called the *Yamabe equation*. By solving the Yamabe equation, one can design a conformal metric $e^{2u}\mathbf{g}$ with a prescribed curvature $\bar{K}$.

The Yamabe equation can be solved using the *Ricci flow* method. The Ricci flow deforms the metric $\mathbf{g}(t)$ according to the Gaussian curvature $K(t)$ (induced by itself), where t is the time parameter

$$\frac{dg_{ij}(t)}{dt} = 2(\bar{K} - K(t))g_{ij}(t).$$

The *uniformization theorem* [15] for surfaces says that any metric surface admits a Riemannian metric of constant Gaussian curvature, which is conformal to the original metric. Such metric is called the *uniformization metric*.

Poincaré disk model In this work, we use the Poincaré disk to model the hyperbolic space $\mathbb{H}^2$, which is the unit disk $|z| < 1$ in the complex plane with the metric $ds^2 = \frac{4dzd\bar{z}}{(1-z\bar{z})^2}$. The rigid motion is the Möbius transformation

$$z \to e^{i\theta}\frac{z - z_0}{1 - \bar{z}_0 z},$$

where θ and z_0 are parameters. The geodesics on the Poincaré disk are arcs of Euclidean circles, which intersect the boundary of the the unit circle at right angles.

Suppose S is a surface with a negative Euler number, and its hyperbolic uniformization metric is $\tilde{\mathbf{g}}$. Then its universal covering space $(\tilde{S}, \tilde{\mathbf{g}})$ can be isometrically embedded in $\mathbb{H}^2$. Any deck transformation of $\tilde{S}$ is a Möbius transformation, which is a transformation from one universal covering space to another universal covering space and keeps projection invariant, and called a *Fuchsian transformation*. The deck transformation group is called the *Fuchsian group* of S.

Let ϕ be a Fuchsian transformation, let $z \in \mathbb{H}^2$, the *attractor* and *repulser* of ϕ are $\lim_{n\to\infty}\phi^n(z)$ and $\lim_{n\to\infty}\phi^{-n}(z)$ respectively. The *axis* of ϕ is the unique geodesic through its attractor and repulser.

Teichmüller Space Let $(S_1, \mathbf{g}_1)$ and $(S_2, \mathbf{g}_2)$ be two metric surfaces, and let $f : S_1 \to S_2$ be a differential map between them. If the pull-back metric induced by f satisfies the following condition:

$$\mathbf{g}_1 = e^{2\lambda} f^* \mathbf{g}_2,$$

then we say the map is *conformal*. Two metric surfaces are conformally equivalent, if there exists an invertible conformal map between them. All surfaces may be classified using this conformal equivalence relation.

All conformal equivalence classes of surface with a fixed topology form a finite-dimensional manifold, the so-called Teichmüller space. Teichmüller space is a shape space, where a point represents a class of surfaces, and a curve in Teichmüller space represents a deformation process from one shape to the other. The coordinates of the surface in Teichmüller space can be explicitly computed. The Riemannian metric of The Teichmüller space is also well-defined.

In this work, only genus-zero surfaces with three boundaries are considered, which are also called as *topological pants*. Let $(S, \mathbf{g})$ be a pair of topological pants with a Riemannian metric $\mathbf{g}$, with three boundaries

$$\partial S = \gamma_1 + \gamma_2 + \gamma_3.$$

Let $\tilde{\mathbf{g}}$ be the uniformization metric of S, such that the Gaussian curvature is equal to -1 at every interior point, and the boundaries are geodesics. If the length of the boundary γ_i is l_i under the uniformization metric, then (l_1, l_2, l_3) are the Teichmüller coordinates of S in the Teichmüller space of all conformal classes of a pair of pants. Namely, if two surface share the same Teichmüller coordinates, they can be conformally mapped to each other.

Figure 1 (a) illustrates a pair of pants with the hyperbolic metric, such that the three boundaries, $\gamma_i, i = 1 - 3$, are geodesics. The τ_i are the shortest geodesics connecting γ_j, γ_k, so τ_i is orthogonal to both γ_j and γ_k. The γ_i are divided to two segments with equal lengths by τ_j, τ_k. τ_1, τ_2 and τ_3 split the surface to two identical hyperbolic hexagons, with edge lengths $\frac{\gamma_1}{2}, \tau_3, \frac{\gamma_2}{2}, \tau_1, \frac{\gamma_3}{2}, \tau_2$. Furthermore, all the internal angles are right angles. The lengths of τ_1, τ_2, τ_3 are determined by $\gamma_1, \gamma_2, \gamma_3$. For the mapping in Figure 1 (a) to be made, the pair of pants can have any geometry, as long as it has the topology shown. It helps us to study general brain anatomical structures.

3. Computational Algorithms

This section details the algorithms for computing the hyperbolic metric, and the Teichmüller coordinates.

3.1. Hyperbolic Ricci Flow Algorithm

In practice, most surfaces are approximated by discrete triangular meshes. Let M be a two-dimensional simplicial complex. We denote the set of vertices, edges and faces by V, E, F respectively. We call the ith vertex v_i; edge $[v_i, v_j]$ runs from v_i to v_j; and the face $[v_i, v_j, v_k]$ has its vertices sorted counter-clockwise. Figure 1 (b) shows the hyperbolic triangle, and its associated edge lengths l_i, y_i, corner angles θ_i and conformal factors u_i.

A *discrete metric* is a function $l : E \to \mathbb{R}^+$, such that triangle inequality holds on every face, which represents the edge lengths. In this work, we assume all faces are hyperbolic triangles. The *discrete curvature* $K : V \to \mathbb{R}$ is defined as the angle deficit, i.e., 2π minus the surrounding corner angles for an interior vertex, and π minus the surrounding corner angles for a boundary vertex.

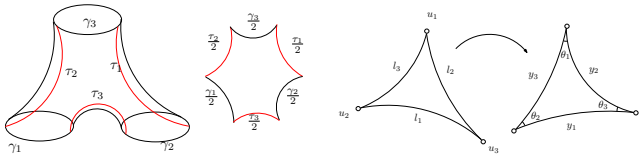

(a) (b)

Figure 1. (a). A pair of hyperbolic pants. (b) Discrete surface Yamabe flow.

3.1.1 Discrete conformal deformation

Suppose the mesh is embedded in $\mathbb{R}^3$, so it has the induced Euclidean metric. We use l_{ij}^0 to denote the initial induced Euclidean metric on edge $[v_i, v_j]$.

Let $u : V \to \mathbb{R}$ be the *discrete conformal factor*. The discrete conformal metric deformation is defined as

$$\sinh(\frac{y_k}{2}) = e^{u_i} \sinh(\frac{l_k}{2}) e^{u_j}. \tag{1}$$

The *discrete Yamabe flow* is defined as

$$\frac{du_i}{dt} = -K_i, \tag{2}$$

where K_i is the curvature at the vertex v_i.

Let $\mathbf{u} = (u_1, u_2, \cdots, u_n)$ be the conformal factor vector, where n is the number of vertices, and $\mathbf{u_0} = (0, 0, \cdots, 0)$. Then the *discrete hyperbolic Yamabe energy* is defined as

$$E(\mathbf{u}) = \int_{\mathbf{u_0}}^{\mathbf{u}} \sum_{i=1}^{n} K_i du_i. \tag{3}$$

The differential 1-form $\omega = \sum_{i=1}^{n} K_i du_i$ is closed. We use c_k to denote $\cosh(y_k)$. By direct computation, it can be shown that on each triangle,

$$\frac{\partial \theta_i}{\partial u_j} = A \frac{c_i + c_j - c_k - 1}{c_k + 1},$$

where

$$A = \frac{1}{\sin(\theta_k) \sinh(y_i) \sinh(y_j)},$$

which is symmetric in i, j, so $\frac{\partial \theta_i}{\partial u_j} = \frac{\partial \theta_j}{\partial u_i}$. It is easy to see that $\frac{\partial K_i}{\partial u_j} = \frac{\partial K_j}{\partial u_i}$, which implies $d\omega = 0$. The discrete hyperbolic Yamabe energy is convex. The unique global minimum corresponds to the hyperbolic metric with zero vertex curvatures.

This requires us to compute the Hessian matrix of the energy. The explicit form is given as follows:

$$\frac{\partial \theta_i}{\partial u_i} = -A \frac{2c_i c_j c_k - c_j^2 - c_k^2 + c_i c_j + c_i c_k - c_j - c_k}{(c_j + 1)(c_k + 1)}$$

The Hessian matrix (h_{ij}) of the hyperbolic Yamabe energy can be computed explicitly. Let $[v_i, v_j]$ be an edge, connecting two faces $[v_i, v_j, v_k]$ and $[v_j, v_i, v_l]$. Then the edge weight is defined as

$$h_{ij} = \frac{\partial \theta_i^{jk}}{\partial u_j} + \frac{\partial \theta_i^{lj}}{\partial u_j}.$$

also for

$$h_{ii} = \sum_{j,k} \frac{\partial \theta_i^{jk}}{\partial u_i},$$

where the summation goes through all faces surrounding v_i, $[v_i, v_j, v_k]$.

The discrete hyperbolic energy can be directly optimized using Newton's method. Because the energy is convex, the optimization process is stable.

Given the mesh M, a conformal factor vector $\mathbf{u}$ is *admissible* if the deformed metric satisfies the triangle inequality on each face. The space of all admissible conformal factors is not convex. In practice, the step length in Newton's method needs to be adjusted. Once the triangle inequality no longer holds on a face, then an edge swap needs to be performed.

3.2. Algorithm for Computing the Teichmüller Coordinates

Figure 2 illustrates the major steps for computing the Teichmüller space coordinates. Frame (a) illustrates the input metric surface with three boundaries γ_1, γ_2, and γ_3. Frame (b) and (c) illustrate the curve τ_1, which connects γ_2, γ_3, and τ_2 connecting γ_1, γ_3. Then we slice the surface S along τ_1 and τ_2 to obtain a simply connected surface, $\tilde{S}$. By running the hyperbolic Yamabe flow, the hyperbolic metric is obtained. $\tilde{S}$ then can be isometrically embedded onto the Poincaré disk as shown in frame (d). The boundaries of the original surface $\gamma_1, \gamma_2, \gamma_3$ map to geodesics. In frame (d), the Möbius transformation ϕ_1 that transforms τ_1 to τ_1^{-1}

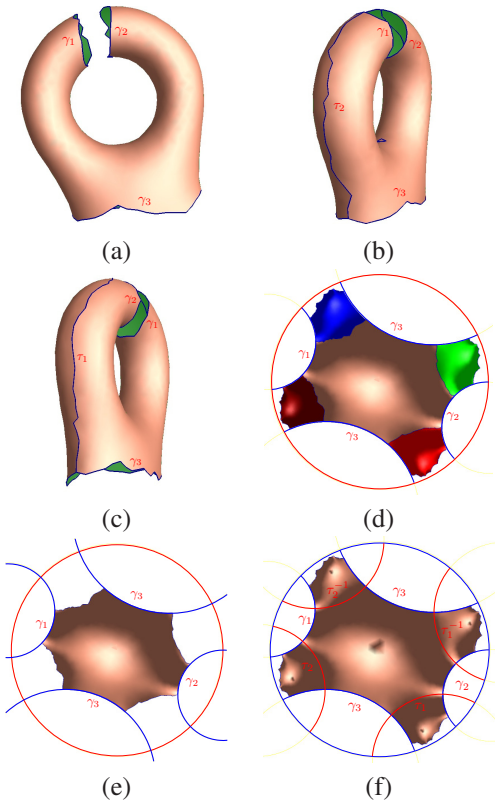

Figure 2. Computing Teichmüller coordinates.

can be directly computed. Similarly the Möbius transformation ϕ_2 can also be easily computed, which maps τ_2 to τ_2^{-1}. Then $\{\phi_1, \phi_2\}$ are the generators of the Fuchsian group of S. In frame e, the embedding of $\tilde{S}$ in the hyperbolic disk is transformed by a Fuchsian transformation. Each color represents one copy of $\tilde{S}$, transformed by a Fuchsian transformation. Frame (f) shows the computation of the τ_i's, which are the shortest geodesics connecting the geodesic boundaries γ_j, γ_k.

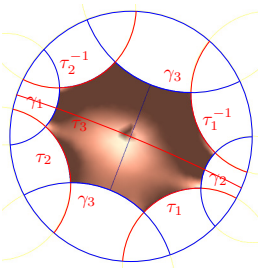

Figure 3. A Poincaré disk embedding for Teichmüller space coordinate computation.

The final result is shown in Figure 3. The original surface is separated by τ_1, τ_2, τ_3 into two right-angled hyperbolic hexagons. The edge lengths of the hexagon are $\frac{\gamma_1}{2}, \tau_2, \frac{\gamma_3}{2}, \tau_1, \frac{\gamma_2}{2}, \tau_3$.

4. Experimental Results

We applied our shape analysis to various anatomical surfaces extracted from 3D MRI scans of the brain. In this paper, the segmentations are regarded as given, and result from automated and manual segmentations detailed in other prior works, e.g. Chou et al. [3] and Thompson et al. [17].

4.1. Application to Studying Brain Surface Morphometry

Figure 4 (a)-(b) illustrate the Teichmüller space coordinate computation on a left hemisphere cortical surface with 3 selected landmark curves: the Central Sulcus, Superior Temporal Sulcus, and Primary Intermediate Sulcus. After we cut a cortical surface open along the selected landmark curves, a cortical surface becomes topologically equivalent to a genus-zero surface with three open boundaries. The surface is topologically equivalent to the topological pant surface (Figure 1 (a)). We can compute its conformal parameterization to the Poincaré disk with the hyperbolic Ricci flow and further compute its Teichmüller space coordinate. (a)-(b) illustrates a cortical surface and its embedding in the Poincaré disk. The three boundaries are labeled as γ_i and two shortest geodesics that connect boundaries are labeled as τ_i.

Lots of studies have associated accelerated dilation of the cerebral ventricles with risk for and progression of HIV/AIDS, dementia and MCI in elderly subjects [17, 2, 6, 3]. Ventricular changes reflect atrophy in surrounding structures, and ventricular measures and surface-based maps can provide sensitive assessments of tissue reduction that correlate with cognitive deterioration in illnesses. However, the concave shape, complex branching topology and narrowness of the inferior and posterior horns have made automatic analyses more difficult. To model the lateral ventricular surface, we automatically locate and introduce three cuts on each ventricle. The cuts are motivated by examining the topology of the lateral ventricles, in which several horns are joined together at the ventricular "atrium" or "trigone". We call this topological model, creating a set of connected surfaces, a *topology optimization* operation. After modeling the topology in this way, a lateral ventricular surface, in each hemisphere, becomes an open boundary surface with 3 boundaries, a topological pant surface.

After the topology optimization, a ventricular surface is topologically equivalent to a topological pant surface. We can then compute its Teichmüller space coordinate. Figure 4 illustrates how to compute Teichmüller space coordinates for a lateral ventricle. In the figure, γ_1, γ_2, and γ_3 are labeled boundaries and τ_1 and τ_2 are the shortest geodesics between boundaries. Figure 4 (b) illustrates the surface with

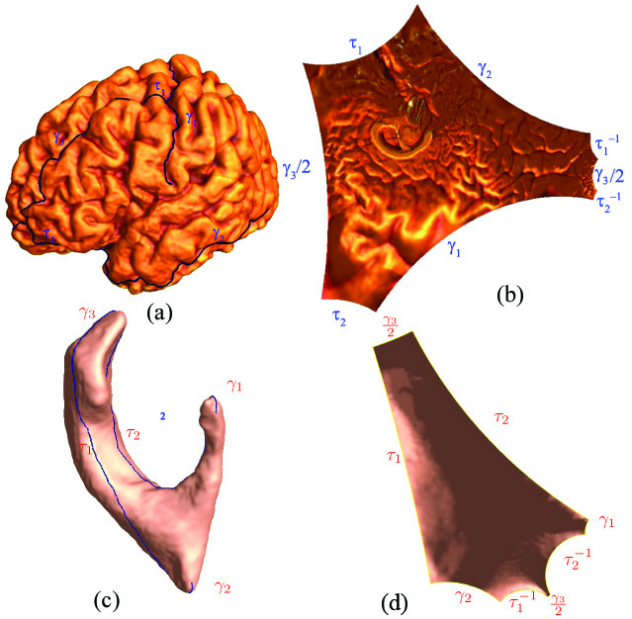

Figure 4. Computing Teichmüller space coordinates for a cortical surface and a ventricle surface. (a) is a left hemisphere cortical surface with 3 selected landmark curves. (b) shows the cortical surface is isometrically flattened to the Poincaré disk. (c) and (d) illustrate a ventricular surface with labeled boundaries and its Poincaré disk flattening result.

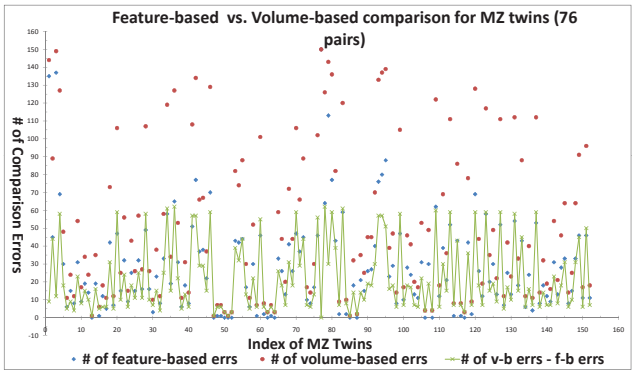

(a)

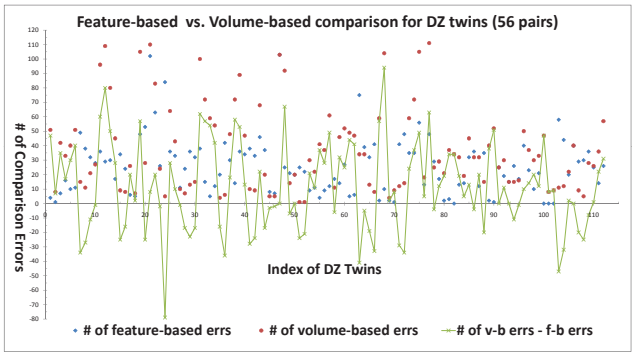

(b)

Figure 5. Comparison of shape feature based algorithm and volume measure based algorithm to study genetic influence on ventricular shape in twins. (a) is the result on identical twin group and (b) is on same-sex fraternal twin group. The Teichmüller space based shape index captures reported a lower number of comparison errors. It may indicate that the Teichmüller space based shape index may be more useful to detect genetic effects than volume measures.

the hyperbolic metric that is isometrically flattened onto the Poincaré disk. When we make the topological change, we make sure each new boundary has the same Euclidean length across different surface. As a result, the lengths of each boundary under the Poincaré disk metric are valid metrics for studying lateral ventricular surface morphometry.

4.2. Genetic Influences on Ventricular Structure in Twins

We analyzed ventricular shapes in 3D volumetric MRI scans from 76 identical and 56 same-sex fraternal twins, scanned as part of a 5-year research project [3]. For each ventricular surface, we computed its Teichmüller space coordinates as a 3×1 vector. With the L^2 norm, we hypothesized that our shape index could help find each subjects twin pair in the database, assuming it has a closer shape index than the rest of surfaces.

In a preliminary research, we compared our shape index with volume measures. For a given ventricular surface, we computed and sorted the distances to all other ventricular surfaces. Then we counted how many "wrong" ventricular surface that has a shorter distance than the one to its twin peer. We called this number as the *number of comparison errors* associated with the ventricular surface. We define the *error rate* as the ratio of the error number and the number of all surfaces compared. We computed the comparison errors for each ventricular surface with our shape index and volume measures. Figure 5 illustrates the number of comparison errors of two shape measures for all ventricular surfaces on 76 identical twins (MZ) and 56 same-sex fraternal twins (DZ). We also calculate the difference of number of comparison errors of volume measure and that of shape index measure. From the figure, we can learn that shape index feature did a better job than volume feature for MZ twin data because all volume feature error numbers are larger than the shape index error numbers. For 76 identical twins, the median error rate was 14.3% (versus 24.7% error rate for volume measures). For 56 same-sex fraternal twins, the median error rate was 22.3% (versus 26.4% error rate for volume measures). We also compared the number of comparison errors between each pair of twins and found that the median and mean of comparison errors between pairs of identical twins were consistently less than those of fraternal twins. This suggests that the Teichmüller space based shape

index may be more useful to detect genetic effects than volume measures.

4.3. Lateral Ventricle Shape Analysis of HIV/AIDS

In another experiment, we compared ventricular surface models extracted from 3D brain MRI scans of 11 individuals with HIV/AIDS and 8 control subjects [17]. We automatically perform topology optimization on each ventricular surface and compute their lengths in the Poincaré disk by the Yamabe flow method. For each pair of ventricular surfaces, we obtained a 6×1 vector, $t = (t_1, t_2, ...t_6)$, which consists of 3 boundary lengths for the left ventricular surface and 3 boundary lengths for right ventricular surface. Given this Teichmüller space coordinate based feature vector, we apply a nearest neighbor classifier based on the Mahalanobis distance, which is

$$\begin{aligned} d(t) &= \sqrt{(t-\mu_{T_c})^T \Sigma_{T_c}^{-1} (t-\mu_{T_c})} \\ &+ \sqrt{(t-\mu_{T_a})^T \Sigma_{T_a}^{-1} (t-\mu_{T_a})} \end{aligned}$$

where μ_{T_c}, μ_{T_a}, Σ_{T_c} and Σ_{T_a} are the feature vector mean and covariance for the two groups, respectively. We classify t based on the sign of the distance of $d(t)$, i.e., the subject that is closer to one group mean is classified into that group. For this data set, we performed a leave-one-out test. Our classifier successfully classified all 19 subjects to the correct group and achieved a 100% accuracy rate [18].

For comparison, we also tested a nearest neighbor classifier associated with a volume feature vector. For each pair of ventricular surface, we measure their volumes, (v_l, v_r). We also use a nearest neighbor classifier based on the Mahalanobis distance, which is

$$\begin{aligned} d(v) &= \sqrt{(v-\mu_{V_c})^T \Sigma_{V_c}^{-1} (v-\mu_{V_c})} \\ &+ \sqrt{(v-\mu_{V_a})^T \Sigma_{V_a}^{-1} (v-\mu_{V_a})} \end{aligned}$$

where μ_{V_c}, μ_{V_a}, Σ_{V_c} and Σ_{V_a} are the feature vector mean and covariance two groups, respectively. We classify v based on the sign of the distance of $d(v)$, i. e., the subject that is closer to one group mean is classified into that group. In the data set, we performed a leave-one-out test. The classifier based on the simple volume measurement successfully classified only 13 out of 19 subjects to the correct group and achieved a 68.42% accuracy rate.

Figure 6 shows an interesting experimental result. Two pairs of lateral ventricular surfaces, are shown, from (a) a healthy control individual, and (b) from an individual with HIV/AIDS. Both of them have highly irregular shapes. Although generally HIV/AIDS makes the lateral ventricle dilate, here the ventricle from the control group has a bigger volume than the one from the HIV/AIDS group on both sides. The volume differences between these two subjects are about 0.62% and 5.2% of the mean left and right side volumes in the whole data set. The volume-based classifier assigned all of these ventricular surfaces to the incorrect diagnostic groups while the Teichmüller space coordinate based classifier classified each of them correctly.

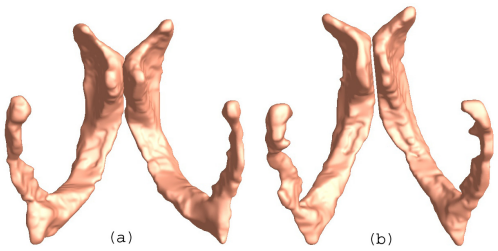

Figure 6. Lateral ventricular surfaces of a control subject (a) and an individual with HIV/AIDS. The volume of lateral ventricular surface of the control subject is greater than that of the HIV/AIDS individual. Our Teichmüller space coordinate feature successfully classified these surfaces, when entered into a nearest neighbor classifier. The volume measurement based nearest neighbor classifier achieved a 68.42% accuracy rate.

Studies of ventricular morphometry have also used 3D statistical maps to correlate anatomy with clinical measures, but automated ventricular analysis is still difficult because of their highly irregular branching surface shape. The new Teichmüller space shape descriptor requires more validation on other data sets, these experimental results suggest that (1) ventricular surface morphometry is altered in HIV/AIDS; (2) volume measures are not sufficient to distinguish HIV patients from controls; and (3) our Teichmüller space feature vector can be used to classify control and patient subjects. Our ongoing work is studying the correlation between the proposed feature vector and clinical measures (e.g., future decline) in an Alzheimer's Disease data set.

5. Conclusion and Future Work

In this paper, we propose a stable way to compute Teichmüller space coordinate for a surface with a certain type of branching topology. We applied it as a shape index to study brain morphometry for genetic shape analysis and HIV/AIDS. We included our shape index in a nearest neighbor classifier that correctly classified all lateral ventricle surfaces from 8 control and 11 HIV/AIDS individuals (versus only 68% accuracy rate for volume measure). Although our current work focuses on topological pant surfaces, for surfaces with more complicated topologies, their Teichmüller coordinates can still be computed using the hyperbolic metric. If the surface has Euler number χ, $\chi < 0$, the surface can be decomposed to $-\chi$ number of pants, where the cutting curves are also geodesics under the hyperbolic metric.

Furthermore, two pants sharing a common cutting curve can be glued together with a specific twisting angle. The lengths of all cutting geodesics and the twisting angles associated with them form the Teichmüller coordinates of the surface. In the future, we will further explore and validate numerous applications of the Teichmüller shape space in neuroimaging and shape analysis research.

Acknowledgement: This work was funded by National Institute of Health through the NIH Roadmap for Medical Research, Grant U54 RR021813 entitled Center for Computational Biology (CCB).

References

[1] C. M. Botino, C. C. Castro, R. L. Gomes, C. A. Buchpiguel, R. L. Marchetti, and M. R. Neto. Volumetric MRI measurements can differentiate Alzheimer's disease, mild cognitive impairment and nomral aging. *International Psychogeriatrics*, 14:59–72, 2002.

[2] O. T. Carmichael, P. M. Thompson, R. A. Dutton, A. Lu, S. E. Lee, J. Y. Lee, L. H. Kuller, O. L. Lopez, H. J. Aizenstein, C. C. Meltzer, Y. Liu, A. W. Toga, and J. T. Becker. Mapping ventricular changes related to dementia and mild cognitive impairment in a large community-based cohort. *Biomedical Imaging: Nano to Macro, 2006. 3rd IEEE International Symposium on*, pages 315–318, April 2006.

[3] Y. Chou, N. Leporé, M. Chiang, C. Avedissian, M. Barysheva, K. L. McMahon, G. I. de Zubicaray, M. Meredith, M. J. Wright, A. W. Toga, and P. M. Thompson. Mapping genetic influences on ventricular structure in twins. *NeuroImage*, 44(4):1312 – 1323, 2009.

[4] M. Chung, K. Dalton, and R. Davidson. Tensor-based cortical surface morphometry via weighted spherical harmonic representation. *IEEE Trans. Med. Imag.*, 27(8):1143–1151, Aug. 2008.

[5] R. H. Davies, C. J. Twining, P. D. Allen, T. F. Cootes, and C. J. Taylor. Shape discrimination in the hippocampus using an MDL model. In *Proc. Infor. Proc. Med. Imag. (IPMI)*, 2003.

[6] L. Ferrarini, W. M. Palm, H. Olofsen, M. A. van Buchem, J. H. Reiber, and F. Admiraal-Behloul. Shape differences of the brain ventricles in Alzheimer's disease. *NeuroImage*, 32(3):1060 – 1069, 2006.

[7] K. Gorczowski, M. Styner, J.-Y. Jeong, J. Marron, J. Piven, H. Hazlett, S. Pizer, and G. Gerig. Statistical shape analysis of multi-object complexes. *IEEE Conf. Comp. Vis. Patt. Recog. CVPR '07*, pages 1–8, June 2007.

[8] X. Gu, S. Wang, J. Kim, Y. Zeng, Y. Wang, H. Qin, and D. Samaras. Ricci flow for 3D shape analysis. *Computer Vision, 2007. ICCV 2007. IEEE 11th International Conference on*, pages 1–8, Oct. 2007.

[9] H. W. Guggenheimer. *Differential Geometry*. Dover Publications, 1977.

[10] A. Hatcher. *Algebraic Topology*. Camerbirdge University Press, 2006.

[11] M. Jin, W. Zeng, F. Luo, and X. Gu. Computing Teichmüller shape space. *IEEE Trans. Vis. Comput. Graphics*, 15(3):504–517, 2009.

[12] I. Kakadiaris, G. Passalis, G. Toderici, M. Murtuza, Y. Lu, N. Karampatziakis, and T. Theoharis. Three-dimensional face recognition in the presence of facial expressions: An annotated deformable model approach. *IEEE Trans. Pattern Anal. and Machine Intell.*, 29(4):640–649, April 2007.

[13] S. Li, F. Shi, F. Pu, X. Li, T. Jiang, S. Xie, and Y. Wang. Hippocampal shape analysis of Alzheimer's disease based on machine learning methods. *American J. of Neuroradiology*, 28:1339–45, 2007.

[14] S. Pizer, D. Fritsch, P. Yushkevich, V. Johnson, and E. Chaney. Segmentation, registration, and measurement of shape variation via image object shape. *IEEE Trans. Med. Imag.*, 18(10):851–865, Oct. 1999.

[15] R. Schoen and S.-T. Yau. *Lectures on Differential Geometry*. International Press, 1994.

[16] P. Thompson and A. Toga. A surface-based technique for warping 3-dimensional images of the brain. *IEEE Trans. Med. Imag.*, 15(4):1–16, 1996.

[17] P. M. Thompson, R. A. Dutton, K. M. Hayashi, A. Lu, S. E. Lee, J. Y. Lee, O. L. Lopez, H. J. Aizenstein, A. W. Toga, and J. T. Becker. 3D mapping of ventricular and corpus callosum abnormalities in HIV/AIDS. *NeuroImage*, 31(1):12–23, 2006.

[18] Y. Wang, W. Dai, T. F. Chan, S.-T. Yau, A. W. Toga, and P. M. Thompson. Teichmüller shape space theory and its application to brain morphology. In *Med. Image Comp. Comput.-Assist. Intervention, Proceedings*, 2009.

[19] Y. Wang, X. Gu, T. F. Chan, P. M. Thompson, and S.-T. Yau. Brain surface conformal parameterization with algebraic functions. *Med. Image Comp. Comput.-Assist. Intervention, Proceedings, Part II*, pages 946–954, 2006. LNCS 4191.

[20] W. Zeng, X. Yin, Y. Zeng, Y. Lai, X. Gu, and D. Samaras. 3D face matching and registration based on hyperbolic Ricci flow. *CVPR Workshop on 3D Face Processing 2008*, pages 1–8, 23-28 June 2008.